PHYSICAL REVIEW B **92**, 020509(R) (2015)

Scalable architecture for quantum information processing with superconducting flux qubits based on purely longitudinal interactions

P.-M. Billangeon,[1,2,*] J. S. Tsai,[1,3] and Y. Nakamura[1,2]
[1] *RIKEN Center for Emergent Matter Science (CEMS), 2-1 Hirosawa, Wako, Saitama 351-0198, Japan*
[2] *Research Center for Advanced Science and Technology (RCAST), The University of Tokyo, Meguro-ku, Tokyo 153-8904, Japan*
[3] *Department of Physics, Faculty of Science, Tokyo University of Science, Shinjuku-ku, Tokyo 162-8601, Japan*

(Received 14 January 2015; revised manuscript received 4 June 2015; published 20 July 2015)

We devise a quantum register based on superconducting flux qubits that circumvents the impediments posed by the presence of fixed interactions. We describe a coupling scheme wherein two physical qubits are coupled to a third which acts as a *coupler* via their longitudinal degree of freedom (i.e., σ_z). This approach provides a solution to several issues such as residual interactions between physical qubits, deteriorations of the rotating wave approximation (RWA), and correlated errors, thereby expanding the opportunities for capitalizing on the large coupling strengths achievable with these systems.

DOI: 10.1103/PhysRevB.92.020509 PACS number(s): 03.67.Lx, 85.25.Cp

Josephson-junction-based qubits are promising candidates in the quest for a scalable quantum information processing hardware, owing to the prospect of integrating these circuits into large-scale systems [1]. Other advantages include the large attainable coupling strengths [2,3] and the versatility of controlling and reading out the quantum state of these devices. A generic issue in solid-state devices is the potential adverse effect of fixed interactions between qubits [4]. The resulting residual $\sigma_z\sigma_z$ interactions (e.g., Ref. [5]) lower the fidelity of single- and two-qubit gates as the resonant frequency of each physical qubit depends on the state of its neighbors and cause a constant accumulation of spurious phase along the targeted unitary evolution. The justification of the RWA is another concern, as is the emergence of various types of correlated errors due to the combined effect of qubit decoherence and fixed couplings. The latter aspect finds its most well-known manifestation with the Purcell effect in cavity/circuit QED [6–8].

Here, we aim at developing a quantum register free of such restrictions. We consider a layout based on a two-dimensional (2D) array of physical qubits on a square lattice, which is the basis for the implementation of the surface code [9]. We previously presented a comprehensive review of circuit QED architectures wherein microwave resonators mediate the interaction between physical qubits, thereby allowing us to dispose the latter farther apart from one another and, in so doing, mitigate cross-talk [10]. This Rapid Communication is focused on densely arranged quantum registers, which is decidedly relevant from a practical point of view considering the high overhead inherent to quantum error correction.

Several proposals discuss how to implement tunable interactions at the level of two qubits, based on direct or mediated interactions [11–20]. However, a careful analysis of the limitations that arise at large scale and a systematic approach to counteracting them are still lacking. Here, we consider a different strategy wherein each pair of nearest-neighboring physical qubits are longitudinally coupled to a coupler via its longitudinal degree of freedom.

This type of Hamiltonian involving only interactions between the longitudinal degree of freedom of the qubits is reminiscent of that encountered in nuclear magnetic resonance (NMR) quantum information processing [21,22]. However, it should be noted that the $\sigma_z\sigma_z$ interactions found in NMR systems correspond to an approximation of the Heisenberg interaction between nuclear spins via J coupling in the limit where the coupling is small compared with the Zeeman splitting. In the case of three-junction flux qubits with a gradiometric design, a pure $\sigma_z\sigma_z$ interaction can be obtained without any restriction on the coupling strength by defining an inductive coupling between the currents flowing in the loops defined by splitting the smaller junction (α-junction) of each qubit in a SQUID geometry (so-called α-loop) as depicted in Fig. 1(a) [23–25]. Another noteworthy asset of this device is its large anharmonicity compared with most other Josephson-junction-based artificial atoms, such that the two-level approximation is well justified. Whether the improving trend of coherence properties of transmons and Xmons [26–29] may apply to flux qubits is currently under investigation [30–32].

Static Hamiltonian. In the aforementioned configuration, the Hamiltonian of a unit cell is

$$\mathcal{H}_{\text{cell}} = -\sum_{i=1,2,c} \frac{\Delta_i}{2}\sigma_i^z + \frac{J_{1c}}{2}\sigma_1^z\sigma_c^z + \frac{J_{2c}}{2}\sigma_2^z\sigma_c^z, \qquad (1)$$

where Δ_i is the resonant frequency of each qubit and J_{ic} is the coupling strength between each physical qubit and the coupler. Henceforth, we will parameterize the coupling strengths as $J_{1c} = J(1+\rho)$ and $J_{2c} = J(1-\rho)$, where ρ is a parameter characterizing the asymmetry between the coupling strengths J_{ic} linking the physical qubits to the coupler. A noteworthy advantage of this system is that its Hamiltonian is already diagonal, which is the key to overcoming most of the aforementioned limitations. The resonant frequency ω_i of each physical qubit is independent of the state of the other owing to the absence of residual $\sigma_z\sigma_z$ interaction between them, while ω_i is renormalized by the interaction with the coupler [see Fig. 1(b)]. Provided that the coupler lies in its ground state,

*Author to whom all correspondence should be addressed: pierre.billangeon@gmail.com

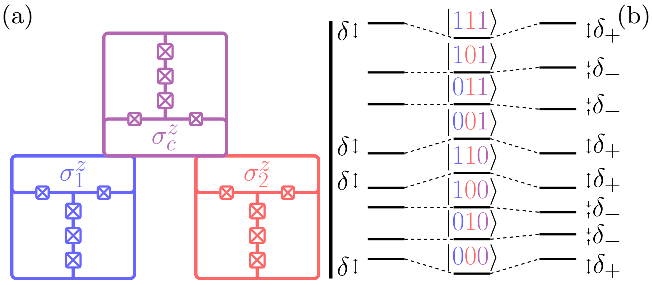

FIG. 1. (Color online) (a) Schematic representation of three gradiometric flux qubits all coupled via their longitudinal degree of freedom [ZZZ configuration]. This type of interaction can be achieved in a configuration wherein all qubits are inductively coupled by means of their α-loop. (b) Associated energy level diagram of the bare qubits ($J = 0$, center), with symmetric couplings ($\rho = 0$, left), and arbitrary couplings (right).

ω_i is given by $(\Delta_i - J_{ic})/\hbar$. Interestingly, this Hamiltonian is parity conserving as the coupling terms trivially commute with the parity operator ($[\mathcal{H}, \Pi_{3q}] = 0$ where $\Pi_{3q} = \sigma_1^z\sigma_2^z\sigma_c^z$). This ensures that transitions between states of the same parity are forbidden under the transverse microwave drive of the physical qubits or the coupler by virtue of the parity selection rule, which stands as an advantage as it alleviates the difficulty of justifying the RWA by eliminating unwanted terms which may occur at higher order.

Controlled-phase gate. The dependence of the resonant frequency of the coupler on the state of the physical qubits [see Fig. 1(b)] can serve as a basis for a mechanism of conditional phase accumulation, allowing us to implement a controlled-phase (C_φ) gate in a single step. Assuming that we apply a transverse microwave drive to the coupler, the corresponding time-dependent Hamiltonian is thus given by

$$\mathcal{H}_{\mathrm{cell}}(t) = \mathcal{H}_{\mathrm{cell}} + \Omega_c(t)\cos(\omega_c t + \phi_c)\sigma_c^x, \tag{2}$$

where $\mathcal{H}_{\mathrm{cell}}$ is given by Eq. (1), and Ω_c, ω_c, and ϕ_c are the amplitude, the frequency, and the phase of the microwave drive, respectively. In order to switch to the rotating frame of the two physical qubits and the coupler, we apply the time-dependent unitary transformation

$$\mathcal{U} = \prod_{i=1,2,c} \exp\left[\mathrm{i}\,\frac{(\omega_i t + \phi_i^{\mathrm{ref}})}{2}\,\sigma_i^z\right], \tag{3}$$

where $\omega_1 = (\Delta_1 - J_{1c})/\hbar$, $\omega_2 = (\Delta_2 - J_{2c})/\hbar$, and ϕ_i^{ref} are the reference phases of the rotating frame of each qubit.

Without loss of generality, we set $\phi_c = \phi_c^{\mathrm{ref}} = 0$. We thus obtain the time-dependent Hamiltonian below:

$$\mathcal{H}'_{\mathrm{cell}}(t) = \sum_{i=1,2,c} \frac{\delta_i}{2}\,\sigma_i^z + \frac{J_{1c}}{2}\,\sigma_1^z\sigma_c^z + \frac{J_{2c}}{2}\,\sigma_2^z\sigma_c^z + \frac{\Omega_c(t)}{2}[(1 + \mathrm{e}^{\,\mathrm{i}\,2\omega_c t})\sigma_c^+ + (1 + \mathrm{e}^{-\mathrm{i}\,2\omega_c t})\sigma_c^-], \tag{4}$$

where $\delta_i = (\hbar\omega_i - \Delta_i)$ are the detunings.

The validity of the RWA is ensured as it is in the case of an isolated qubit (i.e., the Bloch-Siegert oscillations can be ignored if $\Omega_c \ll 2\,\hbar\omega_c$). Within the RWA, the effective Hamiltonian is found to be

$$\mathcal{H}_{\mathrm{cell}}^{\mathrm{RWA}} = \sum_{i=1,2,c} \frac{\delta_i}{2}\,\sigma_i^z + \frac{J_{1c}}{2}\,\sigma_1^z\sigma_c^z + \frac{J_{2c}}{2}\,\sigma_2^z\sigma_c^z + \frac{\Omega_c(t)}{2}\,\sigma_c^x. \tag{5}$$

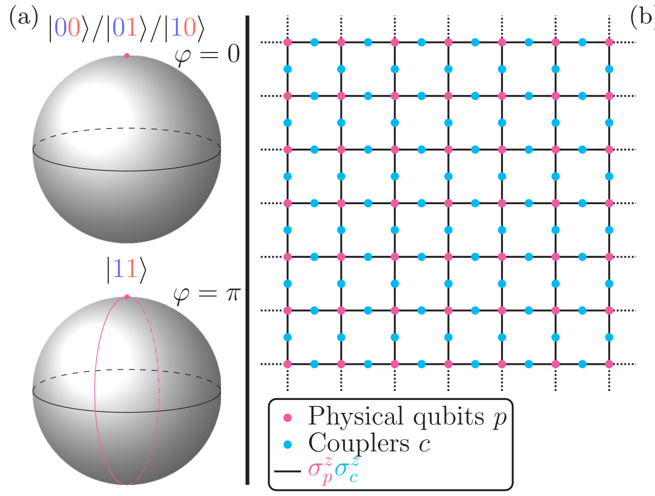

FIG. 2. (Color online) (a) Idealized evolution of the coupler in the Bloch sphere representation depending on the state of the physical qubits during a coupler drive pulse (2π pulse) at the frequency $(\Delta_c + 2J)/h$. We assume that $\Omega \ll (1 - |\rho|)(2J)$. (b) Schematic representation of an array of qubits on a 2D square lattice wherein each physical qubit is coupled via its longitudinal degree of freedom to its nearest neighbors through the intermediary of the longitudinal degree of freedom of a coupler.

Let us assume that we apply a 2π pulse to the coupler at the frequency $(\Delta_c + 2J)/h$ in the limit where the strength of the microwave drive is sufficiently small compared with the effective detuning $(1 - |\rho|)(2J)$ between the state $|11\rangle$ and either the state $|10\rangle$ ($\rho \geqslant 0$) or $|01\rangle$ ($\rho \leqslant 0$). If the physical qubits are in the state $|11\rangle$, the coupler will perform a full rotation on the Bloch sphere and accumulate a global phase π, otherwise it will remain in the ground state provided that the effective detuning is large compared with the Rabi frequency, as schematically depicted in Fig. 2(a). This mechanism of conditional phase accumulation has the merit of directly generating a C_φ gate, without the need for additional single-qubit operations and without requiring a precise adjustment of the phase of the microwave drive applied to the coupler. This approach extends a class of mechanisms of conditional phase accumulation via an avoided crossing with a state outside of the computational subspace [12,33–35] to artificial atoms with a large anharmonicity. This scheme can also be compared with the controlled-NOT gate proposed by Barenco *et al.* [36], the difference being that our approach does not utilize direct $\sigma_z\sigma_z$ interactions between physical qubits, thus ensuring its scalability.

We perform numerical calculations to determine the fidelity of the C_φ gate based on a Lie algebraic method [37] and the exact time-dependent Hamiltonian [see Eq. (4)]. We consider the initial state $|\psi_0\rangle = 1/2\,(|0_1 0_2 0_c\rangle + |0_1 1_2 0_c\rangle + |1_1 0_2 0_c\rangle + |1_1 1_2 0_c\rangle)$. We examine the case where the microwave pulse applied to the coupler has a Gaussian envelope whose half-width

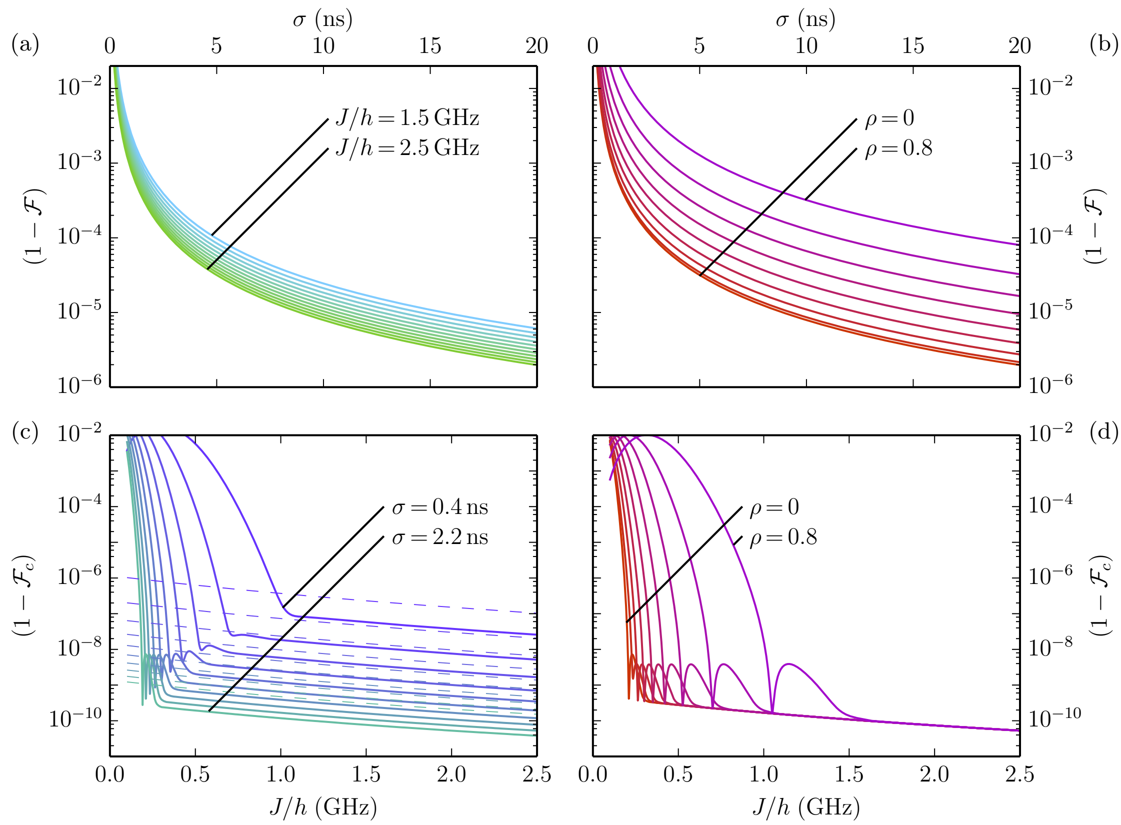

FIG. 3. (Color online) Top: overall infidelity $(1-\mathcal{F})$ of the C_φ gate against the microwave pulse duration σ for different values of (a) the average coupling strength J ($\Delta_c/h = 6\,$GHz, $\rho = 0$, and J/h ranges from 1.5 to 2.5 GHz in steps of 0.1 GHz) and (b) the asymmetry parameter ρ ($\Delta_c/h = 6\,$GHz, $J/h = 2.5\,$GHz, and ρ ranges from 0 to 0.8 in steps of 0.1). Bottom: infidelity $(1-\mathcal{F}_c)$ with which the coupler is brought back in its ground state against the average coupling strength J for different values of (c) the pulse length σ ($\Delta_c/h = 6\,$GHz, $\rho = 0$, and σ ranges from 0.4 to 2.2 ns in steps of 0.2 ns) and (d) the asymmetry parameter ρ ($\Delta_c/h = 6\,$GHz and $\sigma = 2\,$ns). For comparison, we plot the fidelity associated with a Rabi flop for an isolated qubit with the same resonant frequency $(\Delta_c + 2J)/h$, and a Gaussian pulse with the same length [dashed curves in (c)].

σ characterizes the speed of the two-qubit operation [38]. We determine the overall fidelity $\mathcal{F}$ of the entire process [i.e., $\mathcal{F} = |\langle\psi_\mathrm{f}|\psi_\mathrm{t}\rangle|^2$ where $|\psi_\mathrm{f}\rangle$ is the final state of the three-qubit system after the pulse and $|\psi_\mathrm{t}\rangle = 1/2\,(|0_1 0_2 0_c\rangle + |0_1 1_2 0_c\rangle + |1_1 0_2 0_c\rangle - |1_1 1_2 0_c\rangle)$ is the targeted state]. We establish values that are compatible with the implementation of the surface code for rather short microwave pulses (namely with σ of the order of a few nanoseconds). The fidelity $\mathcal{F}$ is an increasing function of the pulse length σ [see Figs. 3(a) and 3(b)] and the average coupling strength J [see Fig. 3(a)], in accordance with the lower ratio of the amplitude of the microwave drive to the effective detuning. We also find that the fidelity $\mathcal{F}$ is a decreasing function of the asymmetry parameter ρ for a given set of parameters σ and J [see Fig. 3(b)], which we attribute to the corresponding reduced effective detuning $(1-|\rho|)(2J)$.

We determine the fidelity $\mathcal{F}_c$ characterizing the closeness of the state of the coupler to its ground state at the end of the pulse [i.e., $\mathcal{F}_c = |\langle\psi_c|0_c\rangle|^2$ where $|\psi_c\rangle$ is the state of the coupler subsequent to the pulse]. We observe two different regimes depending on whether or not the relation between the strength of the microwave drive and the effective detuning $(1-|\rho|)(2J)$ invalidates the selective excitation of the coupler [see Fig. 2(a)]. In the low-J limit, the values of the infidelity $(1-\mathcal{F}_c)$ are rather high and show a strong deviation from the case of an isolated qubit [see dashed curves in Fig. 3(c) for comparison]. This disparity signifies that the risk of generating residual entanglement between the physical qubits and the coupler is greatly enhanced and that the system should not be operated in this regime. However, in the large-J limit we find that for a given pulse length σ, the infidelity $(1-\mathcal{F}_c)$ exhibits a rather flat dependence as a function of J: The plateau corresponding thereto displays a small negative slope for increasing values of J, consistent with the increased accuracy of the RWA as the ratio $\Omega_c/(\Delta_c + 2J)$ decreases.

The unwanted entanglement between the physical qubits and the coupler manifests itself through the discrepancy between the fidelity $\mathcal{F}_c$ for a coupler included among a unit cell, and an isolated qubit with equivalent parameters [see the solid and dashed curves in Fig. 3(c), respectively]. Accordingly, this entangling gate comes with some leakage of information out of the computational subspace; however, the loss of information can be made arbitrary low by adjusting the length of the applied microwave pulse, as reflected in the dependence of the infidelity $(1-\mathcal{F}_c)$ on σ [see Fig. 3(c)].

Correlated errors. The main benefit of this scheme relies on the fact that the static Hamiltonian is already diagonal [see Eq. (1)], meaning that the eigenstates are the bare states. This implies that fixed interactions under the effect of either qubit relaxation or dephasing do not introduce correlated errors, which is advantageous from the standpoint of error correction.

The holistic picture. We address the issue of the applicability of the RWA for both single- and two-qubit operations within the frame of a large-scale quantum register, as depicted in Fig. 2(b). Besides the parity selection rule, which still applies for such a lattice, the fully diagonal static Hamiltonian simplifies the task.

We categorize the qubits depending on whether they are physical qubits ($i \in p$) or couplers ($i \in c$). The time-dependent Hamiltonian of an entire 2D array, including the transverse microwave drive applied to the physical qubits (single-qubit operations) and the couplers (two-qubit operations), is given by

$$\mathcal{H}_{\text{array}}(t) = -\sum_{i\in\{p,c\}} \frac{\Delta_i}{2}\sigma_i^z + \sum_{\langle i,j\rangle} \frac{J_{ij}}{2}\sigma_i^z\sigma_j^z + \sum_{i\in\{p,c\}} \Omega_i(t)\cos(\omega_i t + \phi_i)\sigma_i^x, \tag{6}$$

where $\langle i,j\rangle$ denotes the summation over all pairs of nearest neighbors, and Ω_i, ω_i, and ϕ_i are, respectively, the amplitude, the frequency, and the phase of the microwave drive applied to each qubit. In order to switch to the rotating frame of all the qubits belonging to the array, we apply the time-dependent unitary transformation

$$\mathcal{U} = \prod_{i\in\{p,c\}} \exp\left[\mathrm{i}\,\frac{(\omega_i t + \phi_i^{\text{ref}})}{2}\sigma_i^z\right] \quad \text{where}$$
$$\omega_i = \Delta_i/\hbar - \sum_{\substack{j\in c\\ \langle i,j\rangle}} J_{ij}/\hbar \quad \text{if} \quad i \in p,$$
$$\omega_i = \Delta_i/\hbar + \sum_{\substack{j\in p\\ \langle i,j\rangle}} J_{ij}/\hbar \quad \text{if} \quad i \in c, \tag{7}$$

and ϕ_i^{ref} are the reference phases of the rotating frame of each qubit. The resulting time-dependent Hamiltonian of the quantum register reads

$$\mathcal{H}'_{\text{array}}(t) = \sum_{i\in p} \frac{\delta_i}{2}\sigma_i^z + \sum_{j\in c} \frac{\delta_j}{2}\sigma_j^z + \sum_{\langle i,j\rangle} \frac{J_{ij}}{2}\sigma_i^z\sigma_j^z + \sum_{i\in\{p,c\}} \frac{\Omega_i(t)}{2}[(\mathrm{e}^{\mathrm{i}(\phi_i^{\text{ref}}-\phi_i)} + \mathrm{e}^{\mathrm{i}(2\omega_i t + (\phi_i^{\text{ref}}+\phi_i))})\sigma_i^+ + \text{H.c.}], \tag{8}$$

where H.c. stands for the Hermitian conjugate of the preceding term. The justification of the RWA for single-qubit operations on physical qubits is considerably facilitated by the absence of higher order terms which may entangle them with their surrounding couplers. Accordingly, the RWA does not involve any condition on the detuning between nearest-neighboring qubits in the array [10]; we do not have to envisage the risk to generate spurious entanglement between physical qubits and couplers via cross-resonance [18] or parametric conversion terms [16]. The RWA merely requires that the Bloch-Siegert oscillations are properly averaged out (i.e., $\Omega_i \ll 2\,\hbar\omega_i$), and the same applies to entanglement generation by controlling the coherent dynamics of the couplers as already indicated in the context of a single unit cell. As mentioned above, the mechanism of conditional phase accumulation underlying the two-qubit operations does not require controlling the phase of the microwave drive applied to the couplers. Therefore, for brevity we set $\phi_i = \phi_i^{\text{ref}} = 0$ for the couplers. Within the RWA, the effective Hamiltonian of the entire lattice is given by

$$\mathcal{H}_{\text{array}}^{\text{RWA}} = \sum_{i\in p} \frac{\delta_i}{2}\sigma_i^z + \sum_{j\in c} \frac{\delta_j}{2}\sigma_j^z + \sum_{\langle i,j\rangle} \frac{J_{ij}}{2}\sigma_i^z\sigma_j^z + \underbrace{\sum_{i\in p} \frac{\Omega_i(t)}{2}(\cos(\delta\phi_i)\sigma_i^x - \sin(\delta\phi_i)\sigma_i^y)}_{\text{Single-qubit operations}} + \underbrace{\sum_{j\in c} \frac{\Omega_j(t)}{2}\sigma_j^x}_{\text{Two-qubit operations}}, \tag{9}$$

where $\delta_i = (\hbar\omega_i - \Delta_i)$ are the detunings and $\delta\phi_i = (\phi_i - \phi_i^{\text{ref}})$.

The above effective Hamiltonian is the main result of this work, and despite its simplicity, this coupling scheme solves all the issues discussed so far. All the residual $\sigma_z\sigma_z$ interactions between physical qubits are naturally zero without the necessity of fine-tuning the parameters. The conditions underlying the relevance of the RWA are identical to what they would be for isolated qubits driven resonantly and operated at their symmetry point, thus enabling very fast single- and two-qubit gates. We dub this approach WYAIWYG: What you apply is what you get. We can also infer that the interplay between qubit decoherence and fixed interactions will not induce correlated errors, following the same line of reasoning presented above.

Discussion. Superconducting flux qubits offer a unique testbed for implementing this type of coupling inasmuch as they can support large and pure longitudinal interactions, as opposed to coupled spin systems occurring in NMR-based quantum computation. Coupling physical qubits via their longitudinal degree of freedom enhances their sensitivity to dephasing, which undermines the advantage of operating them at their symmetry point. However, this extra dependence to environmental fluctuations can be counteracted by error suppression [39], while preserving the aforementioned benefits of this scheme at large scale. The combination of all-microwave control and the flexible conditions of applicability of the RWA confer on this coupling scheme a relative robustness against cross-talk, which strengthens its relevance in the context of the large-scale integration of such a compact layout. In spite of the shorter coherence times exhibited by flux qubits to date compared with transmon-based devices, the rather fast single- and two-qubit manipulations allow us to meet the accuracy threshold required for fault-tolerant quantum computation based on the surface code.

Acknowledgments. We gratefully acknowledge discussions with Seth Lloyd, Bill Munro, and Kae Nemoto. P.-M.B. was supported by the RIKEN FPR program. This work was partly funded by the NICT Commissioned Research and ImPACT Program of Council for Science, Technology and Innovation (Cabinet Office, Government of Japan).

[1] M. H. Devoret and R. J. Schoelkopf, Superconducting circuits for quantum information: An outlook, Science **339**, 1169 (2013).

[2] A. O. Niskanen, K. Harrabi, F. Yoshihara, Y. Nakamura, and J. S. Tsai, Spectroscopy of three strongly coupled flux qubits, Phys. Rev. B **74**, 220503(R) (2006).

[3] P. Forn-Díaz, J. Lisenfeld, D. Marcos, J. J. García-Ripoll, E. Solano, C. J. P. M. Harmans, and J. E. Mooij, Observation of the Bloch-Siegert shift in a qubit-oscillator system in the ultrastrong coupling regime, Phys. Rev. Lett. **105**, 237001 (2010).

[4] J. Gea-Banacloche, Qubit-qubit interaction in quantum computers, Phys. Rev. A **57**, R1(R) (1998).

[5] K. Harrabi, F. Yoshihara, A. O. Niskanen, Y. Nakamura, and J. S. Tsai, Engineered selection rules for tunable coupling in a superconducting quantum circuit, Phys. Rev. B **79**, 020507(R) (2009).

[6] E. M. Purcell, Spontaneous emission probabilities at radio frequencies, Phys. Rev. **69**, 681 (1946).

[7] P. Goy, J.-M. Raimond, M. Gross, and S. Haroche, Observation of cavity-enhanced single-atom spontaneous emission, Phys. Rev. Lett. **50**, 1903 (1983).

[8] A. A. Houck, J. A. Schreier, B. R. Johnson, J. M. Chow, J. Koch, J. M. Gambetta, D. I. Schuster, L. Frunzio, M. H. Devoret, S. M. Girvin, and R. J. Schoelkopf, Controlling the spontaneous emission of a superconducting transmon qubit, Phys. Rev. Lett. **101**, 080502 (2008).

[9] A. G. Fowler, M. Mariantoni, J. M. Martinis, and A. N. Cleland, Surface codes: Towards practical large-scale quantum computation, Phys. Rev. A **86**, 032324 (2012).

[10] P.-M. Billangeon, J. S. Tsai, and Y. Nakamura, Circuit-QED-based scalable architectures for quantum information processing with superconducting qubits, Phys. Rev. B **91**, 094517 (2015).

[11] D. V. Averin and C. Bruder, Variable electrostatic transformer: Controllable coupling of two charge qubits, Phys. Rev. Lett. **91**, 057003 (2003).

[12] F. W. Strauch, P. R. Johnson, A. J. Dragt, C. J. Lobb, J. R. Anderson, and F. C. Wellstood, Quantum logic gates for coupled superconducting phase qubits, Phys. Rev. Lett. **91**, 167005 (2003).

[13] J. Lantz, M. Wallquist, V. S. Shumeiko, and G. Wendin, Josephson junction qubit network with current-controlled interaction, Phys. Rev. B **70**, 140507(R) (2004).

[14] C. Rigetti, A. Blais, and M. Devoret, Protocol for universal gates in optimally biased superconducting qubits, Phys. Rev. Lett. **94**, 240502 (2005).

[15] P. Bertet, C. J. P. M. Harmans, and J. E. Mooij, Parametric coupling for superconducting qubits, Phys. Rev. B **73**, 064512 (2006).

[16] A. O. Niskanen, Y. Nakamura, and J. S. Tsai, Tunable coupling scheme for flux qubits at the optimal point, Phys. Rev. B **73**, 094506 (2006).

[17] A. J. Kerman and W. D. Oliver, High-fidelity quantum operations on superconducting qubits in the presence of noise, Phys. Rev. Lett. **101**, 070501 (2008).

[18] C. Rigetti and M. Devoret, Fully microwave-tunable universal gates in superconducting qubits with linear couplings and fixed transition frequencies, Phys. Rev. B **81**, 134507 (2010).

[19] R. A. Pinto, A. N. Korotkov, M. R. Geller, V. S. Shumeiko, and J. M. Martinis, Analysis of a tunable coupler for superconducting phase qubits, Phys. Rev. B **82**, 104522 (2010).

[20] P. C. de Groot, S. Ashhab, A. Lupaşcu, L. DiCarlo, F. Nori, C. J. P. M. Harmans, and J. E. Mooij, Selective darkening of degenerate transitions for implementing quantum controlled-NOT gates, New J. Phys. **14**, 073038 (2012).

[21] N. A. Gershenfeld and I. L. Chuang, Bulk spin-resonance quantum computation, Science **275**, 350 (1997).

[22] D. G. Cory, A. F. Fahmy, and T. F. Havel, Ensemble quantum computing by NMR spectroscopy, Proc. Natl. Acad. Sci. USA **94**, 1634 (1997).

[23] J. E. Mooij, T. P. Orlando, L. Levitov, L. Tian, C. H. van der Wal, and S. Lloyd, Josephson persistent-current qubit, Science **285**, 1036 (1999).

[24] T. P. Orlando, J. E. Mooij, L. Tian, C. H. van der Wal, L. S. Levitov, S. Lloyd, and J. J. Mazo, Superconducting persistent-current qubit, Phys. Rev. B **60**, 15398 (1999).

[25] F. G. Paauw, A. Fedorov, C. J. P. M. Harmans, and J. E. Mooij, Tuning the gap of a superconducting flux qubit, Phys. Rev. Lett. **102**, 090501 (2009).

[26] H. Paik, D. I. Schuster, L. S. Bishop, G. Kirchmair, G. Catelani, A. P. Sears, B. R. Johnson, M. J. Reagor, L. Frunzio, L. I. Glazman, S. M. Girvin, M. H. Devoret, and R. J. Schoelkopf, Observation of high coherence in Josephson junction qubits measured in a three-dimensional circuit QED architecture, Phys. Rev. Lett. **107**, 240501 (2011).

[27] C. Rigetti, J. M. Gambetta, S. Poletto, B. L. T. Plourde, J. M. Chow, A. D. Córcoles, J. A. Smolin, S. T. Merkel, J. R. Rozen, G. A. Keefe, M. B. Rothwell, M. B. Ketchen, and M. Steffen, Superconducting qubit in a waveguide cavity with a coherence time approaching 0.1 ms, Phys. Rev. B **86**, 100506(R) (2012).

[28] J. B. Chang, M. R. Vissers, A. D. Córcoles, M. Sandberg, J. Gao, D. W. Abraham, J. M. Chow, J. M. Gambetta, M. B. Rothwell, G. A. Keefe, M. Steffen, and D. P. Pappas, Improved superconducting qubit coherence using titanium nitride, Appl. Phys. Lett. **103**, 012602 (2013).

[29] R. Barends, J. Kelly, A. Megrant, D. Sank, E. Jeffrey, Y. Chen, Y. Yin, B. Chiaro, J. Mutus, C. Neill, P. O'Malley, P. Roushan, J. Wenner, T. C. White, A. N. Cleland, and J. M. Martinis, Coherent Josephson qubit suitable for scalable quantum integrated circuits, Phys. Rev. Lett. **111**, 080502 (2013).

[30] J. Bylander, S. Gustavsson, F. Yan, F. Yoshihara, K. Harrabi, G. Fitch, D. G. Cory, Y. Nakamura, J. S. Tsai, and W. D. Oliver, Noise spectroscopy through dynamical decoupling with a superconducting flux qubit, Nat. Phys. **7**, 565 (2011).

[31] M. Stern, G. Catelani, Y. Kubo, C. Grezes, A. Bienfait, D. Vion, D. Esteve, and P. Bertet, Flux qubits with long coherence times for hybrid quantum circuits, Phys. Rev. Lett. **113**, 123601 (2014).

[32] J.-L. Orgiazzi, C. Deng, D. Layden, R. Marchildon, F. Kitapli, F. Shen, M. Bal, F. R. Ong, and A. Lupascu, Flux qubits in a planar circuit quantum electrodynamics architecture: Quantum control and decoherence, arXiv:1407.1346.

[33] L. DiCarlo, M. D. Reed, L. Sun, B. R. Johnson, J. M. Chow, J. M. Gambetta, L. Frunzio, S. M. Girvin, M. H. Devoret, and R. J. Schoelkopf, Preparation and measurement of three-qubit

entanglement in a superconducting circuit, Nature (London) **467**, 574 (2010).

[34] T. Yamamoto, M. Neeley, E. Lucero, R. C. Bialczak, J. Kelly, M. Lenander, M. Mariantoni, A. D. O'Connell, D. Sank, H. Wang, M. Weides, J. Wenner, Y. Yin, A. N. Cleland, and J. M. Martinis, Quantum process tomography of two-qubit controlled-Z and controlled-NOT gates using superconducting phase qubits, Phys. Rev. B **82**, 184515 (2010).

[35] J. M. Chow, J. M. Gambetta, A. W. Cross, S. T. Merkel, C. Rigetti, and M. Steffen, Microwave-activated conditional-phase gate for superconducting qubits, New J. Phys. **15**, 115012 (2013).

[36] A. Barenco, D. Deutsch, A. Ekert, and R. Jozsa, Conditional quantum dynamics and logic gates, Phys. Rev. Lett. **74**, 4083 (1995).

[37] J. Wei and E. Norman, Lie algebraic solution of linear differential equations, J. Math. Phys. **4**, 575 (1963).

[38] In the numerical calculations, the temporal extent of the Gaussian envelope of the microwave pulse centered at $t = 0$ was truncated within the time frame $[-5\sigma, 5\sigma]$.

[39] L. Viola and S. Lloyd, Dynamical suppression of decoherence in two-state quantum systems, Phys. Rev. A **58**, 2733 (1998).